

RESEARCH

Open Access



# Biocompatible PLGA-PCL nanobeads for efficient delivery of curcumin to lung cancer

Sheida Sadeghi<sup>1</sup>, Javad Mohammadnejad<sup>2\*</sup>, Akram Eidi<sup>3\*</sup> and Hanieh Jafary<sup>1</sup>

\*Correspondence:  
mohamadnejad@ut.ac.ir;  
eidi@srbiau.ac.ir

<sup>1</sup> Department of Biology, Science and Research Branch, Islamic Azad University, Tehran, Iran

<sup>2</sup> Department of Life Science Engineering, Faculty of New Sciences and Technologies, University of Tehran, Tehran, Iran

<sup>3</sup> Department of Biology, Science and Research Branch, Islamic Azad University, P.O. Box 14515/775, Tehran, Iran

## Abstract

Lung cancer has been mentioned as the first and second most prevalent cancer among males and females worldwide, respectively since conventional approaches do not have enough efficiency in its suppression. Therefore, a biocompatible and efficient poly(lactic-co-glycolic acid) (PLGA: P)- poly( $\epsilon$ -caprolactone) (PCL: P) copolymer was fabricated for delivery of relatively insoluble curcumin (Cur) to A549 lung cancer cells. Next, the physicochemical aspects of the synthesized nanobeads were characterized by applying analytical sets, including FT-IR, DLS, TEM, and TGA as nano-metric size (20–45 nm) and 1.29% of Cur entrapment efficiency were determined for P-P-Cur nano-beads. Thereafter, a controlled (5% within 2 h at pH 7.4) and pH-sensitive (nearly 50% within 4 h at pH 5.0) drug release manner was observed for P-P-Cur nanobeads. Thereafter, biomedical assays were conducted for the cancer suppression ability of nanobeads. 41% cell viability after 24 h of treatment with 200 nM concentration and 7.55% cell cycle arrest at 5 h of post-treatment with 100 nM ( $IC_{50}$ ) concentration were attained for P-P-Cur. Also, 7-fold increase and 2-fold decrease in the expressions of Caspase-9 (apoptotic gene) and Bcl2 (anti-apoptotic gene) were observed which have further approved the cancer inhibition potency of the P-P-Cur sample. The cellular uptake results indicated 91% internalization in A549 cells while it was less than 1% for the pure Cur. These data have demonstrated that P-P-Cur can use as a biocompatible drug delivery system for Cur and treatment of lung cancer.

**Keywords:** PLGA-PCL nanoparticles, Curcumin, Controlled drug release, Drug delivery, Lung cancer inhibition

## Introduction

Cancer, which is one of the most prevalent diseases worldwide, refers to the fast growth and uncontrollable duplication of healthy cells in the body (Shim, et al. 2022; Yousefi et al. 2020). Cancer is considered a significant medical challenge. Cancer cells can extraordinarily develop and destroy normal tissues surrounding the cancer site and result in a big health challenge in the human body (Clinton et al. 2020; He, et al. 2020). The number of patients with cancer and its mortality are going on at an ever-increasing rate as it is predicted that approximately more than 12 million people per year will suffer from cancer by 2030 (Ion et al. 2021). Among different kinds of cancers, lung cancer is reported as the first and second most prevalent cancer among males and females across



the world, respectively (Almurshedi et al. 2018). According to statistics, the death rate of lung cancer is higher than that of the combination of prostate cancer, colorectal cancer, and breast cancer which is an eye-catching report (Xu et al. 2019). As a result, to suppress the ever-increasing rate of cancer prevalence throughout the globe, finding efficient and breakthrough technologies for cancer therapy is required. Nanoparticle-based drug delivery systems (DDS) are contemplated as a great candidate for prognosis, diagnosis, and treatment of cancer rather than traditional approaches, such as thermal therapy, radiotherapy, hormone therapy, surgery, and chemotherapy (Naderlou et al. 2020; Salam et al. 2022; Narmani et al. 2023). Conventional methods in cancer therapy have always been accompanied by some unfavorable drawbacks, like low biocompatibility, considerable side effects, repetitive and long-term treatment period, lack of specificity in cancer targeting, low stability in the human body, applying high drug dosage, high cost, resulting in drug resistance, and so on which have restricted their treatment efficiency (Narmani et al. 2017; Stanicki et al. 2022; Almajidi et al. 2023). To put it in a more vivid picture, chemotherapy, which refers to applying medicines or drugs for cancer therapy, has a remarkable toxic effect on both cancerous and normal cells in the human body. Besides, the prolonged and repetitive treatment periods, administering high drug dosage, inducing the immune system response, inducing multi-drug resistance, anemia, nausea/weight change/dietary issues, less practicality in the elderly, and unaffordability are mentioned as the considerable deficiencies of chemotherapy which sometimes result in lack of efficient treatment and mortality (Almajidi et al. 2024; Saadh et al. 2024). Moreover, surgery is another most common modality in cancer treatment which usually applies along with chemotherapy. Surgery has some remarkable drawbacks, including post-surgery pain at the surgery site, infections at the location of surgery, the possibility of inducing metastasis, and the reaction of the body to the applied drugs to numb the area (local anesthesia), which made it as a less-efficient treatment approach for cancer therapy (Jiang et al. 2023; Amirishoar et al. 2023).

Therefore, using novel and efficient approaches in cancer therapy, such as nanoparticles-based DDS, would be beneficial in many ways (Narmani et al. 2018a; Sarani et al. 2024). Among nanoparticles, polymeric materials owing to a lot of merits, including bioavailability, stability, solubility, tailored and engineered structures, etc., have potentially attracted the attention of researchers and clinicians for the delivery of therapeutics to cancer sites (Hadar et al. 2019). Natural polymers, such as polylactic-co-glycolic acid (PLGA) and poly  $\epsilon$ -caprolactone (PCL), have been approved by the Food and Drug Administration (FDA) for DDSs and clinical applications (Palamà et al. 2017; Zhang et al. 2018). PLGA nanoparticles are composed of lactide and glycolide monomers. Regarding these nanoparticles, there are a number of merits, including appropriate physicochemical aspects, biocompatibility, controlled drug release profile, bioavailability, suitable mechanical strength, good solubility and stability, and so forth which made them a promising platform for efficient DDS (Sheffey et al. 2022; Pelaz et al. 2017). Moreover, easy manipulation and preparation features along with various synthesis approaches and degradation rates have been mentioned as other practical applications of PLGA nanoparticles and introduced as a useful candidate for delivery of bioactive to cancer tissues (Ghitman et al. 2020). On the other hand, PCL, as a member of the aliphatic polyester family, is attained by the polymerization of a monomer and an initiator

at high temperatures (Avramović et al. 2020). The semi-crystalline aspects of PCL (due to high melting point and low glass transition temperature) have led to its regular structure which can degrade in the human body through hydrolyzing ester linkages in its compartment. This degradation indicates its biocompatibility as a practical nanocarrier and places PCL at the top of the practical nanomaterials list (Abrisham et al. 2020; Deng et al. 2019). Semi-crystalline characteristics of PCL have resulted in high stability and durability in the human body which is beneficial for the long-term presence of therapeutics in physiologic serum (Banimohamad-Shotorbani et al. 2021). Besides, degradation of PCL is not accompanied by the production of acidic byproducts in the human body which further verifies the biocompatibility of this polymer. PCL can easily copolymerize with various hydrophobic, hydrophilic, and amphiphilic polymers, such as PEG, chitosan, PLGA, etc., which is an appropriate property for having efficient DDS (Dethe 2022). Both PLGA and PCL nanocarriers can internalize in cancer cells by the enhanced permeability and retention (EPR) effect and epithelial permeability (through opening the tight junctions) (Dethe 2022; Birk et al. 2021).

On the other side, the kind of encapsulated drug, encapsulating capacity, and release rate of DDSs has played a crucial role in cancer treatment efficiency (Khakinahad 2022). Among various therapeutic agents, curcumin (Cur), a natural element derived from the rhizomes of the turmeric plant, is one of the extensively studied therapeutics in many clinical and pre-clinical experiments (Carolina Alves et al. 2019; Patel et al. 2020). Cur can serve as an anti-inflammatory, anti-oxidant, anticancer agent, etc. in medicine (Moutabian 2022). Cur regulates a number of molecular targets in the human cells, such as VEGF (vascular endothelial growth factor), transcription factors (nuclear factor- $\kappa$ B; NF- $\kappa$ B), growth factors like TGF- $\beta$ 1 (tumor growth factor - $\beta$ 1), and TNF- $\alpha$  (tumor necrosis factor- $\alpha$ ) (Shakeri et al. 2019; Tamaddoni et al. 2020). The mechanism of action of Cur can be done intrinsically (mitochondrial) and extrinsically (mediated via cell surface transmembrane death receptors) in target cancer cells (Farghadani and Naidu 2021). Since Cur is water-insoluble (nearly 1.34 mg/L) and unstable in neutral and relatively alkaline pH conditions, its encapsulation in biocompatible hydrophilic compounds such as PLGA-PCL nanocarriers would be promising for the treatment of lung cancer (Carvalho, D.d.M. et al. 2015).

In the present work, we practically synthesized PLGA-PCL nano-beads for delivery of Cur to lung cancer cells. The synthesized nanocarriers were characterized by applying analytical devices, including FT-IR, DLS, TEM, and TGA. Then entrapment efficiency of Cur and its release manner in various pHs were examined. Afterward, biomedical tests, including cell viability, cell cycle arrest, quantitative Real-Time PCR (qRT-PCR), and cellular uptake assays were performed for scrutinizing the ability of nanocarriers in the suppression of lung cancer cells.

## Materials and methods

### Chemicals and apparatus

PLGA (50:50, Mw: 30,000–60,000), PCL (Mw: 14,000 Da), Cur, dichloromethane (DCM), Polyvinyl alcohol (PVA) (M.W. 16 kDa), di-methyl-sulfoxide (DMSO), dichloromethane, dimethyl formamide (DMF), and cellulose dialysis membranes were purchased from Sigma Aldrich. Furthermore, 3-(4,5-dimethylthiazol-2-yl)-2,5-diphenyltetrazolium

bromide (MTT) salt, RPMI 1640 medium, and fetal bovine serum (FBS) were purchased from Sigma-Aldrich. The A549 lung cancer cell lines and the human HGF normal fibroblast cell lines were prepared from the Institute of Pasteur, Iran.

Analytical tests for characterization of synthesized samples were conducted using a NanoDrop 2000c UV-Vis (Thermo scientific), Fourier-transform infrared (FT-IR) (Perkin-Elmer 843), and dynamic light scattering (DLS, NanoBrook 90 Plus, Brookhaven) spectrometer. Also, transmission electron microscopy (TEM) (Philips EM 208S) and thermal gravimetric analysis (TGA) (STA 1500, Rheometric Scientific) were done for analyzing synthesized nanobeads.

#### **Synthesis of PLGA-PCL**

PLGA-PCL nanobeads were prepared using a double emulsion (W/O/W) solvent evaporation approach (Makadia and Siegel 2011). Practically, 10 mg PLGA and 20 mg PCL were separately suspended in 6 ml of DCM (as organic phase) under stirring at 60 rpm and room temperature to obtain an organic solution. Then 5 mL of 1% PVA solution (as aqueous solutions) was prepared and mixed with organic solution (W/O) and emulsified applying a probe-based ultra-sonication at 60% amplitude for 90 s on an ice bag. Thereafter, the prepared emulsion was added to 30 mL of a 1% PVA solution and followed by ultra-sonication at a 60% amplitude for 90 s to form a W/O/W emulsion. Subsequently, the prepared emulsion was stirred for 3 h at room temperature and under vacuum to remove extra DCM. To eliminate PVA, the prepared mixture was rinsed 3 times, centrifuged at 12,000 rpm for 40 min, and consequently, freeze-dried at  $-60^{\circ}\text{C}$  for 3 days to stabilize nanobeads. PLGA-PCL (P-P) was saved at  $4^{\circ}\text{C}$  for analytical and biomedical assessments. This phase of preparation was triplicated.

#### **Synthesis of PLGA-PCL-Cur**

In this section, the double emulsion (W/O/W) solvent evaporation technique was used as same as the previous section. Briefly, 12 mg Cur and 20 mg PLGA-PCL were solubilized in 5 ml of DCM and the mixture was homogenized using a 60 rpm stirring at room temperature. In the following, 5 mL of 1% PVA solution was added to the prepared organic solution followed by emulsification of the mixture using ultra-sonication at 60% set amplitude for 90 s on an ice bag. Next, the prepared emulsion was added to 25 mL of PVA solution (1%) and ultra-sonicated at a 60% amplitude for 90 s. After stirring for 3 h at room temperature, the mixture was put under vacuum conditions and excessive DCM was removed. The formed PLGA-PCL-Cur (P-P-Cur) nanobeads were recovered after washing (3 times) by centrifugation at 12,000 rpm for 40 min to remove the PVA solution and unloaded Cur. Next, the prepared nanobeads were stabilized using a freeze drier at  $-60^{\circ}\text{C}$  for 3 days. Ultimately, the prepared nanobeads were saved at  $4^{\circ}\text{C}$  for analytical and biomedical tests.

#### **Characterization of syntheses**

##### ***FT-IR analysis***

In order to qualify the formation of P-P and also confirm successful Cur loading into nanobeads, the FT-IR was performed in the transmittance mode, using the pellet procedure with KBr, in the wavelength range of  $400\text{--}4000\text{ cm}^{-1}$ . As 4 mg of the samples was

mixed with KBr, compressed into disks using a hydraulic press, and disks were scanned at the mentioned wavelength range.

#### ***DLS and stability analyses***

DLS technique was used to measure the average hydrodynamic size and polydispersity index (PDI) of the synthesized formulations. Briefly, the freshly prepared formulations were sonicated using an ultrasonication set at 37 °C for 15 min to equilibrate the temperature, and the average hydrodynamic size measurements were done at 37 °C in a quartz cuvette at nM concentrations. Also, the size stability of nanobeads was assessed via this analytical approach after incubating their nM concentrations under dark conditions at 4 °C for 21 days.

#### ***TEM analysis***

The particle image and the morphology of the samples were evaluated using TEM. In practice, freshly prepared formulations of nanobeads were dispersed onto a copper grid. After drying samples at 25 °C, the excess liquid was absorbed using a filter paper. The specimens' images were taken at an accelerating voltage of 120 kV. Measurements of the size were taken and averaged (in nm) and micrographs of specimens were attained applying the TEM particle analysis software.

#### ***TGA analysis***

The TGA analysis was conducted for the measurement of thermal stability of P-P and P-P-Cur nanobeads. These measurements were performed under a nitrogen atmosphere using 5 mg of specimens. The temperature ranges from 30 to 800 °C at a heating rate of 10 °C/min in a pan under a constant nitrogen flow rate (40 mL/min) were applied in this analysis.

#### ***Drug release study***

The release profile of Cur from P-P-Cur nanobeads was studied in PBS (simulated in vitro microenvironment of cancer cells). To examine this analysis, a weight equivalent to 3 mg Cur from the freeze-dried P-P-Cur sample was submerged in 5 mL of PBS and spilled in the dialysis tube (sealed from one end) with molecular weight cut-off 12,000 Da. The dialysis tube was pre-soaked in distilled water for 12 h before use. Next, the tube was placed in a beaker containing 100 mL PBS medium under shaking at 120 rpm and temperature of 37 °C. The pH of PBS was also set at 7.4. On the other hand, the same process was done for evaluating drug release in acidic mediums (pH: 5.0 and 6.0) as a simulation of the acidic environment of cancer tissues and cancer cells. Afterward, 10 µL of PBS (release medium) of different pHs was pitted out at various time intervals, including 0.5, 1, 2, 3, 4, 8, 16, 32, and 64 h, and the same amounts of PBS were replaced every time. Eventually, the absorption of the released Cur was quantified at around 420 nm using Nano-drop UV–Vis. The experiments were implemented in triplicate and the percent of the released Cur was calculated.

### Cell culture

The human A549 lung cancer cell line and the human HGF fibroblast normal cells were prepared from the Pasture Institute of Iran. These cell lines were separately cultured in the RPMI medium (Gibco, UK) supplemented with 10% FBS, 2 mM glutamine, 100  $\mu\text{g mL}^{-1}$  streptomycin, and 100 IU  $\text{mL}^{-1}$  penicillin for cellular tests. Cells were eventually incubated at 37 °C and 5%  $\text{CO}_2$  to grow up.

### Cell viability assay

The lung cancer cell growth suppression ability of synthesized nanobeads, including P-P, P-P-Cur, and Cur was studied on A549 and HGF cells after treatment with 50 nM, 100 nM, 150 nM, and 200 nM concentrations using the MTT assay. This test is a rapid quantitative assay that depends on the activity of mitochondrial dehydrogenase to cleave the yellow tetrazolium salt to insoluble purple formazan crystals in viable target cells (Taghavi et al. 2017; Fotouhi et al. 2021). This test was done at 24 h, 48 h, and 72 h of post-treatment times. In practice, the synthesized specimens were first prepared by solubilizing in a serum-supplemented tissue culture medium. Next, the specimens were sterilized using 0.2  $\mu\text{m}$  filtration at pH 7.4. On the other hand, about 5000 cells/100  $\mu\text{L}$  of both A549 and HGF cells were separately seeded in each well of 96-well plates and incubated for 24 h for attachment to the wells. Thereafter, the culture medium of wells was collected, 100  $\mu\text{L}$  of various concentrations of the prepared specimens was spilled in each well, and plates were incubated for 24 h, 48 h, and 72 h. In what follows, after replacing the medium of plates with 200  $\mu\text{L}$  RPMI without serum, 20  $\mu\text{L}$  of sterile-filtered MTT salt prepared in PBS pH 7.4 (5 mg/mL) was added to the wells of the plate, and plates were incubated for 4 h. In the next step, the suspension liquid of wells was collected and 100  $\mu\text{L}$  DMSO was added to each well, and plates were incubated for 20 min. Subsequently, the optical density (OD) (or color intensity) of wells was measured at 570 nm ( $n = 3$ ) and the difference in OD values between the treated and non-treated cells was calculated as cell viability values.

### Cell cycle arrest assay

The cell cycle arrest assay was carried out to study the cell cycle phase and values of cancer cells in the sub- $G_1$  (apoptosis) phase after treatment with  $\text{IC}_{50}$  concentrations of nanobeads. In practice,  $2 \times 10^5$  cells/well of A549 lung cancer cells were seeded in a 6-well plate. Next, after 24 h of incubation of cells for attachment, the  $\text{IC}_{50}$  concentrations of synthesized nanobeads (prepared in a serum-supplemented tissue culture medium) were applied for the treatment of cancer cells for 5 h. Thereafter, the nanocomposite-containing medium was collected, the cells were washed ( $n = 3$ ) with PBS, trypsinized, and rinsed using PBS. Afterward, the cells were transferred to a falcon tube, centrifuged at 3000 rpm for 5 min, and stained using PI. Consequently, cells were incubated under dark circumstances at 4 °C and for 40 min and subjected to flow cytometry to quantify the values of cancer cells in the Sub- $G_1$  phase.

### Gene expression assay

The quantitative Real-Time PCR (qRT-PCR) technique was done to survey the relative expression level of Caspase9 and Bcl2 after 5 h of treatment with IC<sub>50</sub> concentrations of synthesized nanobeads in A549 cells using Q Rotor-Gene (Qiagen, Iran). In practice, the total RNA of cancer cells was isolated as the following procedure. After mixing A549 cells with RNX-PLUS solution, the cells were submerged in 200 µL of chloroform, centrifuged at 13000 rpm for 4 min at 4 °C, and the supernatant was collected. Next, A549 cells were merged with isopropanol, centrifuged at 13000 rpm for 15 min at 4 °C, and the precipitation was collected and the supernatant discarded. Then the precipitation was merged with 1 mL of ethanol 75% to extract RNA. In what follows, cDNA was synthesized using 1000 ng of total RNA by the reverse transcription process. As 10 µL of Master mix real-time, 3 µL (10 ng) RNA, and 7 µL double distilled water were spilled in microtubes for synthesizing cDNA. Thereafter, the qRT-PCR technique was conducted using a 14 µL of the reaction mixture, 1 µL of cDNA, 7 µL of low rox Master mix real-time, and 0.5 µL of forward primer (Caspase-9: 5'TGGCTCCTGGTACGTTGA3'; Bcl2: 5'TCGCCCTGTGGATGACTGA3'; GAPDH: 5'GTGGTCTCCTCTGACTTCAAC3') and 0.5 µL of reverse primer (Caspase-9: 5'GAAACAGCATTAGCGACCCT3'; Bcl2: 5'CAGAGACAGCCAGGAGAAATCA3'; GAPDH: 5'GGAAATGAGGCTTGACAAAGTGG3'). The temperature optimization of PCR was also done by RT-qPCR set as the following: heating at 95 °C for 10 min, 45 cycles at 95 °C for 15 s, annealing at 59 °C for 25 s, and elongation at 72 °C for 30 s. Ultimately, relative gene expression values were normalized to glyceraldehyde-3-phosphate-dehydrogenase (GAPDH) and data were quantified as fold change relative to the control for both genes.

### Cellular uptake

Fluorescein isothiocyanate (FITC)-labeled nanobeads were developed to assess the delivery system in terms of enhanced internalization in the A549 cells as the following procedure. Briefly, the A549 cancer cells were incubated at 37 °C (5% CO<sub>2</sub>) in RPMI (Gibco, UK) medium supplemented with 10% (v/v) FBS, 100 U/mL penicillin, and 1 mg/mL streptomycin. Afterward, 100 nM of Annexin V-binding V-FITC-nanobeads was used for the treatment of A549 cells (1 × 10<sup>6</sup> cells/3 mL) in 6-well plates. This incubation was performed at 37 °C for 40 min. Next, the cells were rinsed with PBS (3 times), collected, and resuspended in PBS buffer. Finally, A549 cells were subjected to the FACS Calibur device (BD Biosciences, CA, USA) for assessment of uptake values.

### Statistical analyses

The experiments were triplicated and outputs were reported as mean ± standard error of the mean. A comparison between groups was analyzed by one-way analysis of variance (ANOVA), and differences were considered significant for \**p* < 0.05.

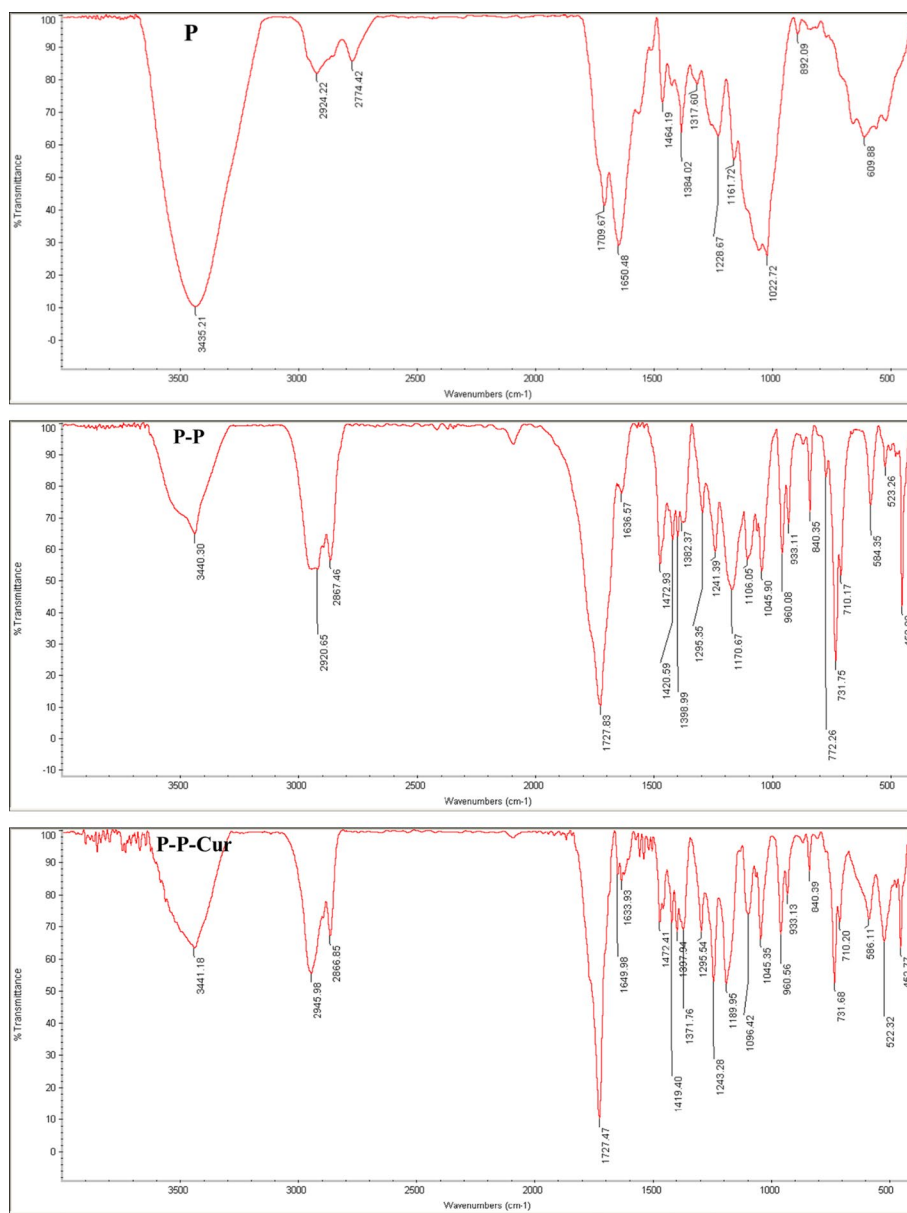


**Fig. 1** FT-IR results of syntheses, including P (PLGA), P-P (PLGA-PCL), and P-P-Cur (PLGA-PCL-Cur). According to the graph of PLGA, wide characteristic peaks at around  $3150\text{--}3650\text{ cm}^{-1}$  are responsible for the  $\text{-OH}$  groups, and the intense characteristic peaks at around  $1650\text{ cm}^{-1}$  and  $1709\text{ cm}^{-1}$  are recorded owing to the stretching vibration of  $\text{C=O}$  groups of PLGA monomers. For the P-P sample, the peaks at around  $3500\text{ cm}^{-1}$  and  $1727\text{ cm}^{-1}$  are assigned due to hydroxyl and ester (carbonyl) groups, respectively. Moreover, the absorption peaks of aliphatic groups are recorded at around  $2920\text{ cm}^{-1}$  ( $\text{O-CH}_3$ ) to  $2866\text{ cm}^{-1}$  ( $\text{O-CH}_2$ ) in P-P nanobeads. Regarding the P-P-Cur sample, the broad peaks at around  $3441\text{ cm}^{-1}$  and  $2945\text{ cm}^{-1}$  are attained owing to the stretching vibration of phenolic  $\text{O-H}$  and aromatic  $\text{C-H}$  stretch vibrations, respectively. The absorption peaks at around  $1633\text{ cm}^{-1}$  and  $1606\text{ cm}^{-1}$  are attributed to  $\text{C=O}$  stretching and aromatic ring stretching of Cur in the compartment of nanobeads

## Results and discussion

### FT-IR analysis

In order to approve the qualification of synthesis and successful Cur loading into P-P, the FT-IR technique was performed for samples, including P, P-P, and P-P-Cur. Figure 1 depicts the results of the FT-IR spectroscopy based on the KBr approach. As can be seen in Fig. 1, a sharp characteristic peak at around  $3150\text{--}3650\text{ cm}^{-1}$  is recorded due to the  $\text{--OH}$  group in the pure PLGA nanoparticles spectrum while the intense absorption peaks at around  $1650\text{ cm}^{-1}$  and  $1709\text{ cm}^{-1}$  are detected owing to the  $\text{C=O}$  groups (stretching vibration) of monomers of PLGA (Abou-ElNour et al. 2019). Moreover, the sharp peaks of  $\text{C--O}$  stretching of ester groups and  $\text{C--H}$  groups in the compartment of PLGA are observed at around  $1022\text{ cm}^{-1}$  and  $1226\text{ cm}^{-1}$ , respectively. Besides, the absorption peaks at around  $2700\text{ cm}^{-1}$  and  $3000\text{ cm}^{-1}$  are responsible for the stretching vibrations of the  $\text{C--H}$  groups in PLGA nanoparticles (Lu et al. 2019). Regarding P-P, the sharp signals of PCL are obtained at around  $3500\text{ cm}^{-1}$  and  $1727\text{ cm}^{-1}$  which are attributed to hydroxyl and ester (carbonyl) groups, respectively (Benkaddour et al. 2013). The sharp characteristic peaks for aliphatic groups are revealed at around  $2920\text{--}2866\text{ cm}^{-1}$  which are due to  $\text{O--CH}_3$  and  $\text{O--CH}_2$  in P-P nanobeads (Yuan et al. 2012). For P-P-Cur nanobeads, the broad peak at around  $3441\text{ cm}^{-1}$  and  $2945\text{ cm}^{-1}$  is attributed to the stretching vibration of phenolic  $\text{O--H}$  and aromatic  $\text{C--H}$  stretch vibrations, respectively. Furthermore, the peaks at around  $1633\text{ cm}^{-1}$  ( $\text{C=O}$  stretching) and  $1606\text{ cm}^{-1}$  (aromatic ring stretching) are responsible for Cur in the body of nanobeads (Ching et al. 2019). The small consecutive peaks of olefinic bending vibration of the  $\text{C--H}$  bond to the benzene ring detected at around  $1490\text{--}1520\text{ cm}^{-1}$  and the peak at around  $1419\text{ cm}^{-1}$  appeared due to  $\text{C--C}$  vibrations.

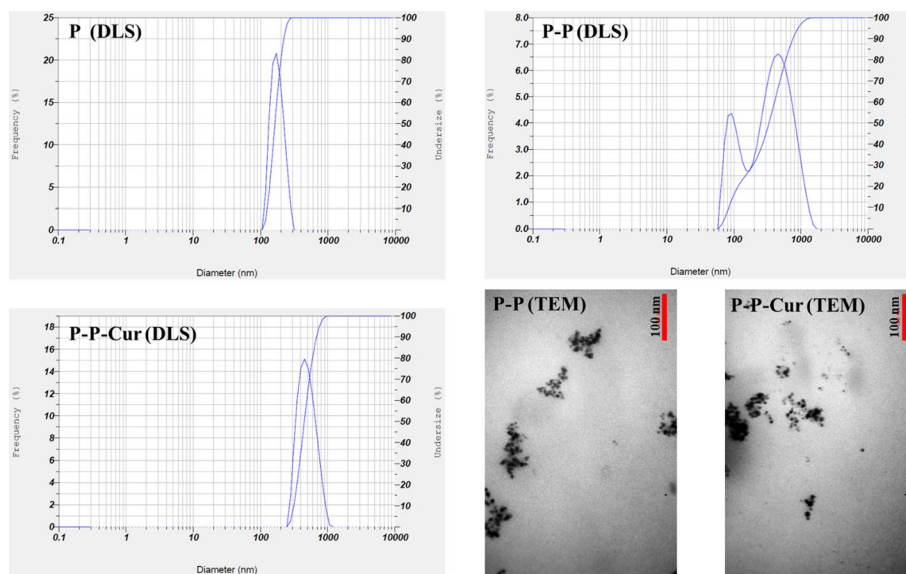


**Fig. 2** DLS and TEM analysis results. According to the results of DLS, the hydrodynamic diameter for pure P (PDI: 0.1), P-P (PDI: 0.18), and P-P-Cur (PDI: 0.13) nanobeads is determined at about 168 nm, 381 nm, and 477 nm, respectively. The TEM images of P-P and P-P-Cur nanobeads show a size range from 40 to 60 nm for the P-P and 60–75 nm for the P-P-Cur sample. The shape of samples is globular and semi-spherical which is suitable for efficient drug delivery to the cancer site

**Table 1** The results of average hydrodynamic diameter, PDI, and diameter stability for the fabricated samples

Fabricated nanobeads	Diameter/nm	PDI	Diameter (nm) after 21 days
P	168 ± 8	0.1 ± 0.03	189 ± 11
P-P	381 ± 10	0.18 ± 0.05	394 ± 13
P-P-Cur	477 ± 14	0.13 ± 0.03	498 ± 8

These assessments were done at 37 °C, pH 7.4, and H<sub>2</sub>O solvent

Additionally, the characteristic peaks corresponding to C=O stretching vibrations attached to the aromatic ring and C–O–C stretching vibrations revealed at around 1280 cm<sup>-1</sup> and 1163 cm<sup>-1</sup>, respectively (Gunathilake et al. 2022).

#### DLS analysis and stability assessment

The hydrodynamic diameter and the polydispersity index (PDI) of synthesized nanobeads, including P, P-P, and P-P-Cur, were analyzed using the DLS technique. Figure 2 and Table 1 demonstrate the results of this technique. Hydrodynamic diameter and PDI have been considered the prominent physicochemical properties of nanocarriers since they can significantly affect pharmacodynamics and pharmacokinetics of DDSs as the circulation, filtration, permeation, and absorption of nanocarriers in cancer sites and cells are directly related to these aspects of DDSs (Mortezaee et al. 2021). According to the results of the DLS device, the hydrodynamic diameter for pure P, P-P, and P-P-Cur nanobeads is determined at about 168 nm, 381 nm, and 477 nm, respectively. These data hint that there is a linear relationship between the copolymerization of nanocarrier and its diameter. As after using PCL, the diameter of nanocarrier is increased by more than 2-fold. Various interactions, such as electrostatic intermolecular interactions and hydrogen bonds, are involved in the compartment of copolymerized DDS (Chen, et al. 2016). The rise in the diameter of P-P-Cur nanobeads could be coordinated with the attachment of Cur to the surface of the nanocarrier by hydrogen bonds. There are other elements, like drug entrapment efficiency, drug release rate, stability, and solubility in the human body serum, etc., which can be affected by the context of a copolymer, PDI, and diameter (Rezvani et al. 2018). The PDI of samples is attained at around 0.1, 0.18, and 0.13 for P, P-P, and P-P-Cur, respectively which indicates relatively homogenized dispersity of synthesized nanobeads. On the other hand, the stability analysis of nanobeads was carried out based on the assessment of diameter using a DLS instrument. This analysis was done after 21 days of incubating nanobeads in dark conditions at 4 °C. As can be seen in Table 1, the diameter of samples indicates small increase as the following order: P nanobeads: from 168 to 189 nm; P-P nanobeads: from 381 to 394 nm; P-P-Cur nanobeads: from 477 to 498 nm. These data present acceptable stability for the long-term storage of nanobeads.

#### TEM analysis

The TEM technique was used to take a visual image of P-P and P-P-Cur nanobeads to confirm their shape, size, dispersion, structure, and morphology (Narmani et al. 2019).

From the TEM images in Fig. 2, it is crystal clear that a size range from 40 to 60 nm and 60 nm to 75 nm is obtained for P-P and P-P-Cur nanobeads, respectively. The morphology and the shape of samples are smooth and spherical and semi-spherical which is appropriate for DDS. As it is reported, the diameter of cancer tissues' vasculatures is in a range from 200 to 700 nm which can preferentially give an allowance to DDSs with a diameter less than 200 nm to infiltrate in the fenestrated blood vessels of the cancer site (Narmani, et al. 2020). The efficient delivery of bioactive to cancer tissues can not only decrease the dose of injected nanocarrier, but can also increase the internalization of DDS into the cancer cells by the EPR effect and pinocytosis pathway. The repetition of treatment times can reduce by having nano-size DDS as well.

### TG Analysis and drug content

In order to scrutinize the Cur content and thermal stability of P-P-Cur and P-P nanobeads, the TGA technique was carried out (Fig. 3). Moreover, the physical status of synthesized nanocarrier has been mentioned to have crucial roles in the down-stream process of the pharmaceutical industry (Dandamudi, et al. 2021). In calculating the drug content of nanocarrier, the weight loss values of TGA curves P-P-Cur and P-P nanobeads were compared to determine the difference between their weight loss values (Narmani

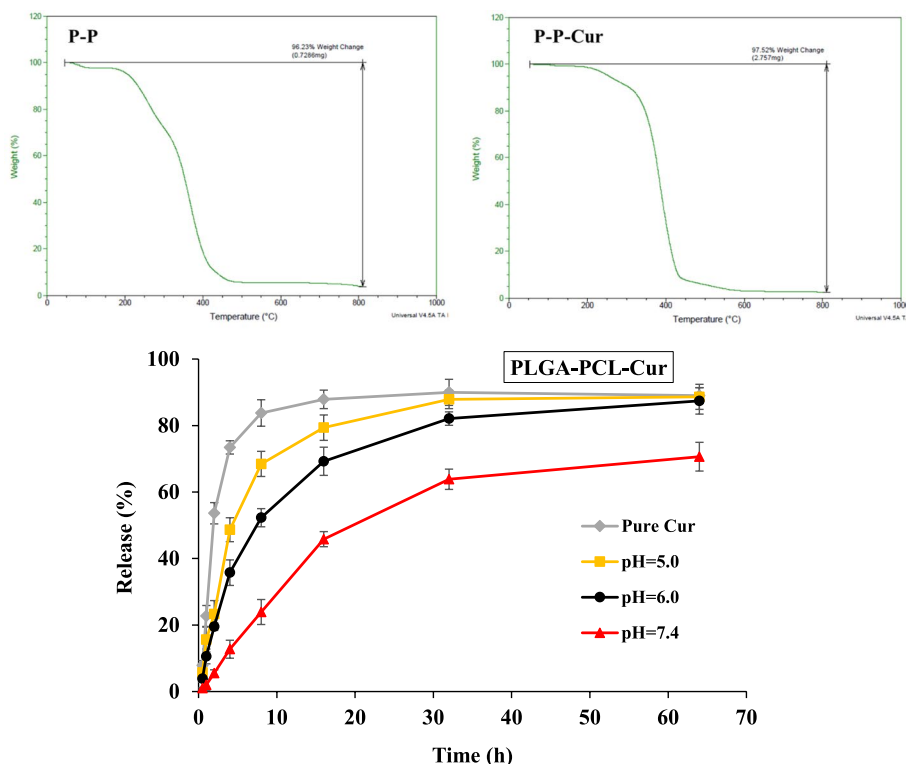


**Fig. 3** Drug content values and drug release profile in acidic and normal pHs. Based on the TGA curves, the total weight loss of P-P and P-P-Cur is recorded at around 96.23 and 97.52%, respectively. By comparing these values, a difference of 1.29% is acquired which refers to drug content. Regarding drug release profile, the burst Cur release is observed within the first 2 h for pure Cur whereas it is just 5% for P-P-Cur in pH 7.4. About 50% of Cur release from P-P-Cur nanobeads is obtained within 20 h at pH 7.4. The pH-sensitive Cur release is recorded for P-P-Cur at pH 6.0 and 5.0 which is appropriate for fast drug release in the acidic microenvironment of cancer tissues

et al. 2018b). This difference is applied to the drug content of P-P-Cur. From Fig. 3, it can be seen that the total weight loss of P-P and P-P-Cur is attained at around 96.23 and 97.52%, respectively which indicates an approximately 1.29% difference in the weight loss values. This amount refers to the drug content of P-P-Cur nanobeads. On the other hand, there are two main weight loss stages in the TGA curves of both samples. The first one is about 3% weight loss at around 90–100 °C (boiling point of water) which coordinates with the water evaporation in both formulations, and the other one is recorded at around 200 °C in which more than 90% weight loss is observed for both samples. This high value of weight loss is associated with the burning of various elements in the compartment of nanobeads.

### Drug release profile

The *in vitro* drug release manner of P-P-Cur nanobeads was carried out in normal (pH: 7.4) and acidic medium (pHs: 5.0 and 6.0) which is similar to the cancerous microenvironment in the human body. Figure 3 shows the release profile of Cur from the nanobeads. As it can be seen, the fast drug release (more than 50%) is recorded within the first 2 h at pH 7.4 for pure Cur while it is only about 5.5% for P-P-Cur under the same circumstances. About 19% and 23% release is attained for pH 6.0 and pH 5.0 after 2 h of incubation, respectively which presents the impact of acidified pH in inducing release rate. After passing 4 h of incubation, the release rate of nanobead is increased to 12% in pH 7.4 which shows more than 2-fold of enhancement compared with its 2 h incubation. This constant release approves the controlled release rate of nanobeads at pH 7.4. In comparison to pH of 7.4, the release rate of nanobead is approximately 3-fold and 4-fold higher in pH 6.0 and 5.0 within the first 4 h, respectively. More than 50% of drug release is observed after 16 h of incubation at normal pH for nanobeads which presents the sustained and controlled drug release (Mariadoss et al. 2022). Copolymerization could effectively decrease the drug rate of nanocarriers which is appropriate for having an efficient DDS. On the other hand, from Fig. 3, it is crystal clear that by increasing the acidity of the release medium, the drug release rate increases which exhibits the pH-sensitive drug release manner of nanocarriers (Narmani and Jafari 2021). To put in a more vivid picture, nearly 20 and 23% of Cur release occurred at pH 6.0 and 5.0 after 2 h of incubation, respectively, whereas it is 5.5% for normal pH. The main reason behind this accelerated drug release manner of nanobeads is acidified pH in protonation side chains of biopolymers, which results in the closing of branches together, opening the nanobead cavities, and maximizing drug release rate. High metabolic rate in cancerous tissues and cells leads to the production of acidic metabolites which change the normal pH to acidic pH in the cancer site. Thus, having a fast drug release rate in acidic environment is favorable for the treatment of cancer (Narmani and Jafari 2021). On the other hand, it is mentioned in reports that the Cur is less prone to crystallize in the emulsions and is stable in them. Cur is more soluble in oil than in water. Moreover, Cur is more stable in acidic pHs, especially in gastric pH, and can be used orally (Kharat et al. 2017). Compared with other polymers, such as polyamidoamine (PAMAM) and polyethylene imine (PEI), our fabricated nanobeads have demonstrated a controlled release manner. For example, compared with a work by Fotouhi et al. in which they developed rituximab functionalized PAMAM-PEG (polyethylene glycol) nanocarrier for controlled delivery

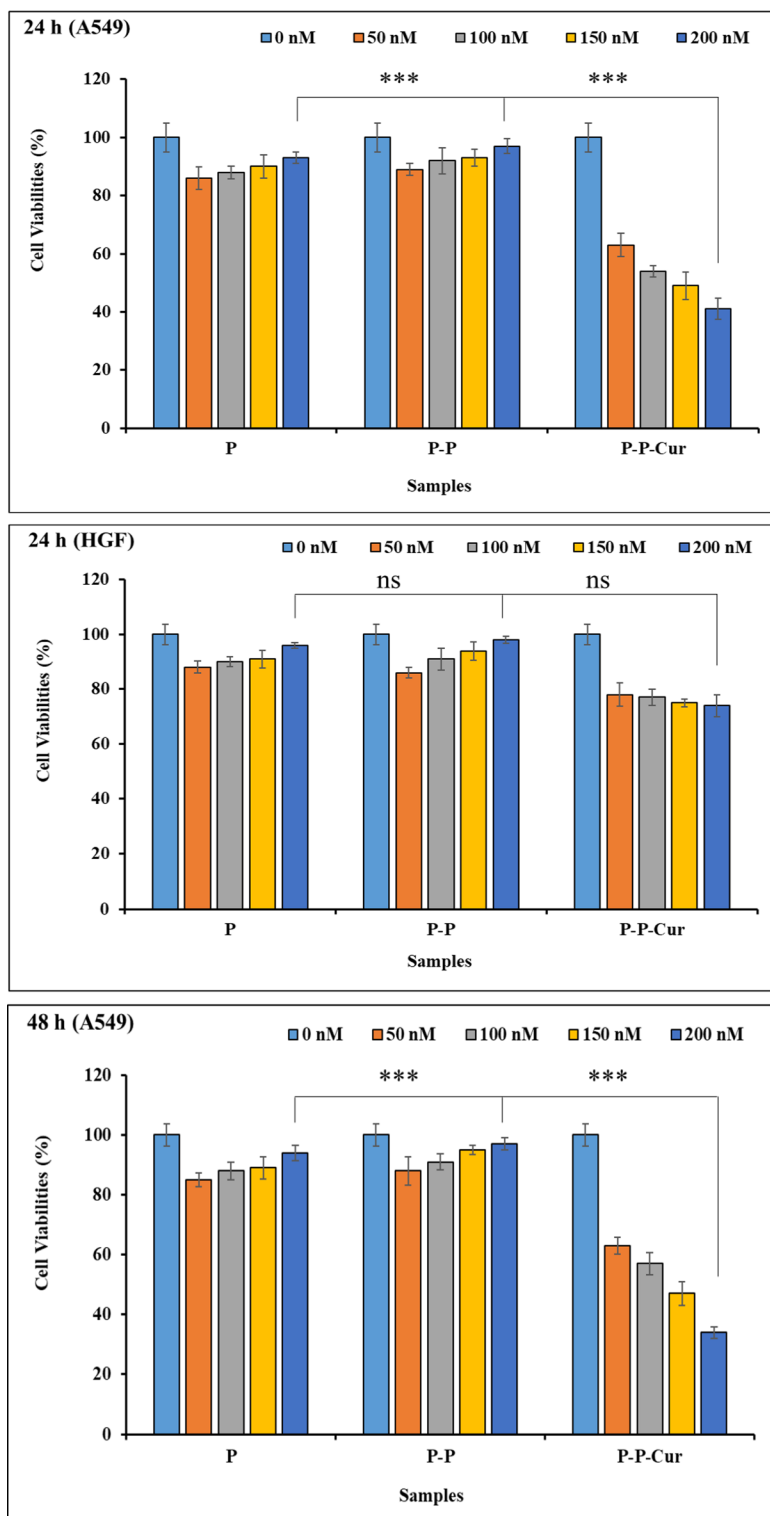


**Fig. 4** Cytotoxic effects of synthesized samples, including P, P-P, P-P-Cur, and Cur, on A549 and HGF cells after 24 h, 48 h, and 72 h of treatment with 50 nM, 100 nM, 150 nM, and 200 nM concentrations. Based on data, around 86 and 93% of cell viabilities are observed for A549 cells after 24 h of treatment with 50 nM and 200 nM concentrations of P samples which presents the biocompatibility and biodegradability of biopolymer. Regarding P-P nano-beads, about 97% cell viability is seen at 200 nM concentration at 24 h of post-treatment while cell viabilities are remarkably declined to 63% and 41% for concentrations of 50 nM and 200 nM after 24 h of treatment, respectively. \* $P < 0.05$ , \*\* $P < 0.01$ , \*\*\* $P < 0.001$ , \*\*\*\* $P < 0.0001$

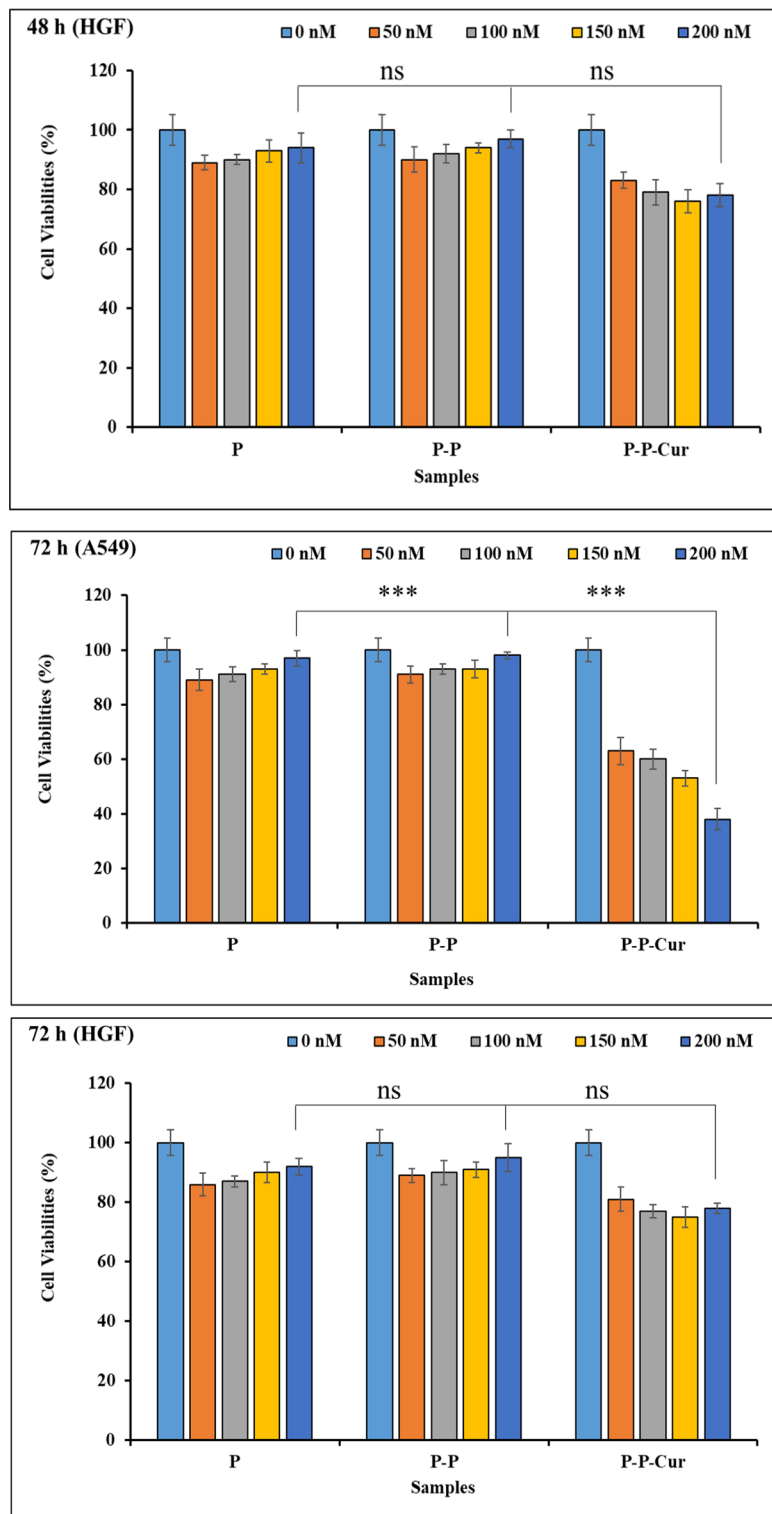


Fig. 4 continued

of imatinib against leukemia cells, our nanobeads have exhibited controlled release manner (Fotouhi et al. 2021). In particular, our nanobead had 12% release within 4 h while it was about 16% for theirs at pH 7.4. Also, while 34% release was detected for their nanocarrier after 8 h of incubation at pH 7.4, it is only 23% for ours.

### Cell viability assay

The MTT test was applied to evaluate the lung cancer cell growth suppression potency of synthesized nanobeads, including P-P, P-P-Cur, and Cur, on A549 and HGF cells after 24 h, 48 h, and 72 h of treatment (Fig. 4). Concentrations of 50 nM, 100 nM, 150 nM, and 200 nM were used in this assay which is kind of rapid quantitative assay based on the activity of mitochondrial dehydrogenase. This enzyme cleaves the yellow tetrazolium salt into insoluble purple formazan crystals in live cells (Fotouhi et al. 2021). As can be seen from Fig. 4, there is a concentration-dependent cell viability values for all samples. By raising the concentrations of P and P-P samples, the cell viability increased which indicates the biocompatibility of biopolymers and copolymerized nanocarrier while the opposite manner in cell viability amounts is true regarding P-P-Cur and Cur samples (Pelaz et al. 2017; Abrisham et al. 2020). To put it in a more vivid picture, 86% and 93% cell viabilities are observed for A549 cells after 24 h of treatment with 50 nM and 200 nM concentrations of P samples which states the biocompatibility and biodegradability of biopolymer. Also, the P-P nanobeads have demonstrated 97% cell viability at 200 nM concentration at 24 h of post-treatment time which further approves the safety of biopolymers for use in DDSs. Approximately the same results are attained for HGF normal cells in different treatment times at various concentrations after treatment with P and P-P specimens (Avramović et al. 2020; Banimohamad-Shotorbani et al. 2021). However, the data for the cell viability values of the P-P-Cur sample in normal cells are significantly different than that of cancer cells. For instance, the cell viability is observed at nearly 80% after 24 h of treatment with 200 nM concentrations of P-P-Cur on normal cells which reveals the biocompatibility of synthesized nanobeads on normal cells. The probable reason for this biocompatibility could be the antioxidant performance of Cur since it has an antioxidant manner at low concentrations in the cytosol of normal cells due to the low rate of metabolism and consequently, low level of uptake rate (Carvalho, D.d.M. et al. 2015). On the other hand, after 24 h of treatment of cancer cells with P-P-Cur nanobeads, the cell viability values are considerably declined to 63% and 41% for concentrations of 50 nM and 200 nM, respectively which exhibits the cytotoxicity of Cur-loaded P-P. The results of pure Cur also expressed the toxic effect on cancer cells, 68% (50 nM) to 48% (200 nM) at 24 h of post-treatment time; however, according to the comparison between pure Cur and P-P-Cur samples, the cancer cell suppression ability of P-P-Cur is remarkably better than that of pure Cur which could be due to the large amounts of long-term and fast drug release after degradation in the acidic medium of late endosomes in the cancer cells (Narmani and Jafari 2021). Cancer cells have a high metabolic rate and can significantly internalize every biocompatible nutrition in the environment through the endocytosis process without being aware of its cargo (Cur). The cell viability results of 48 h and 72 h are as same as that of 24 h in both cell lines. The  $IC_{50}$  value is only acquired for cancer cells, 100 nM (after 24 h and 48 h) and 150 nM (after 72 h) for P-P-Cur and 200 nM for pure Cur in all treatment

times. Our data are in line with the findings of work by Jusu et al. in which they have synthesized a copolymerized PLGA-PEG-PTX (paclitaxel)-LHRH (luteinizing hormone-releasing hormone) biopolymer for the treatment of breast cancer; according to their study, about 80% cell viability was attained after 24 of treatment with 0.5 mg/ mL of P-PEG-PTX-LHRH, whereas it is about 40% after treatment with 200 nM concentration P-P-Cur in our research at the same conditions which present the better performance of our synthesized nanobeads in suppression of cancer cells (Jusu et al. 2020). In another work, Abdouss et al. have developed an H-sensitive nanocarrier based on chitosan-polyacrylic acid-graphitic carbon nitride for the efficient delivery of Cur to breast cancer cells (Abdouss et al. 2023). They used the water/oil/water (W/O/W) emulsification to fabricate the nanocarrier. The cell viability assay indicated that a 5 µg/mL concentration of Cur-containing chitosan-polyacrylic acid-graphitic carbon nitride did lead to about 60% cell viability after 48 h of treatment. Our fabricated nanobeads resulted in less than 40% cell viability at the same incubation time. Besides, in another research by Alizadeh et al., the Cur-entrapped  $\beta$ -cyclodextrin- $\gamma$ -cyclodextrin hollow spheres of chitosan have developed for the treatment of A549 lung cancer cells (Alizadeh and Malakzadeh 2020). They demonstrated that 15, 30, and 45 µg/mL concentrations of Cur-entrapped  $\beta$ -cyclodextrin- $\gamma$ -cyclodextrin hollow spheres of chitosan could result in 61%, 181%, and 91% of inhibition in lung cancer cells, respectively. The best inhibitory function of pure Cur is observed at 15 µg/mL concentration, with about 100% inhibition activity.

### Cell cycle arrest assay

The flow cytometer technique was conducted to scrutinize the cell cycle arrest ability of fabricated nanobeads, including P-P, P-P-Cur, and Cur, in A549 cancer cells. The

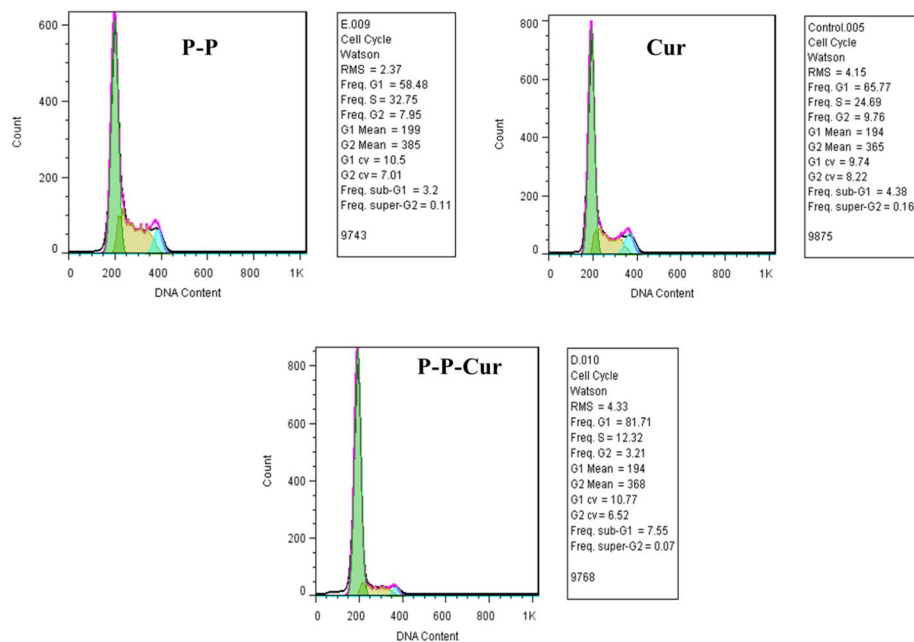


**Fig. 5** The cell cycle arrest outputs after treatment with 100 nM and 150 nM concentrations of nanobeads, including P-P, P-P-Cur, and Cur in A549 cancer cells. The proportion of cancer cells in the apoptotic phase is about 3.2%, 4.38%, and 7.55% for P-P, Cur, and P-P-Cur samples, respectively

100 nM and 150 nM ( $IC_{50}$ ) concentrations of samples were applied to implement this test at 5 h of post-treatment time. Figure 5 exhibits the results of this analysis which is based on the proportion of cells in the sub- $G_1$  phase. This stage of the cell cycle is an indicator of values of cancer cells in the apoptosis phase. From Fig. 5, it can be seen that after treatment of A549 cells with P-P nanobeads, the percent of cells in the sub- $G_1$  phase is approximately 3.2% while after incubations of cancer cells with P-P-Cur sample, the percent of cells in apoptotic phase is increased more than 2-fold and reaches 7.55% which presents the capability of P-P-Cur nanobeads in inducing apoptosis in cancer cells (Moutabian 2022; Shakeri et al. 2019). Moreover, the proportion of cancer cells is about 4.38% after treatment with a 150 nM ( $IC_{50}$ ) concentration of pure Cur which is nearly half of that for the P-P-Cur sample although the 150 nM concentration is used for the treatment of cancer cells compared to 100 nM concentration of P-P-Cur sample. The results of our study are in accordance with the findings of work by Debele et al., in which they have developed glutathione (GSH)-sensitive micelle (PAH-SS-PLGA) loaded with alpha-tocopheryl succinate (TOS) and Cur for the treatment of pancreatic cancer after 48 h of treatment with drug-loaded micelles (at TOS and Cur concentration of 30 and 15  $\mu\text{g}/\text{mL}$ , respectively) (Debele, et al. 2020). Their findings have indicated 45% apoptosis after applying a high concentration of co-delivered nano-complex at 48 h of post-treatment while our results presented low level of apoptosis using a low concentration of a single drug-loaded sample after 24 h of treatment. Furthermore, the results of this study are comparable with the findings of a research by Abdouss et al. in which they developed H-sensitive chitosan-polyacrylic acid-graphitic carbon nitride nanocarrier based on water/oil/water (W/O/W) emulsification approach (Abdouss et al. 2023). This drug delivery system was used for the delivery of Cur against breast cancer cells. They indicated 22% and 17% apoptosis in MCF-7 cells treated with 5  $\mu\text{g}/\text{mL}$  concentration of chitosan-Cur-polyacrylic acid-graphitic carbon nitride and pure Cur after 48 h of incubation, respectively. These results are relatively comparable with the outputs of this study.

#### Gene expression assay

The qRT-PCR technique was implemented to study the relative expression level of Caspase9 and Bcl2 after 5 h of treatment with  $IC_{50}$  concentrations of fabricated nanobeads in A549 cells (Fig. 6). Caspase9 and Bcl2 are pro-apoptotic and anti-apoptotic genes respectively in which their expressions play the prominent role in inducing and suppressing apoptosis in cells. As indicated, the expression level of Caspase9 gene is not significantly changed after treatment with 200 nM concentration of P-P while a relatively 7-fold increase occurs after 100 nM ( $IC_{50}$ ) concentration of P-P-Cur sample which not only depicts the biocompatibility and biodegradability of P-P sample but also shows the extensive impact of Cur-contained nanobeads on suppression of lung cancer cells (Dethe 2022; Farghadani and Naidu 2021). An increase of 2.5-fold in Caspase-9 is recorded for the cells treated with 150 nM ( $IC_{50}$ ) concentration of pure Cur which in comparison to results of the P-P-Cur sample is negligible. The Caspase-9 gene is the member of the cysteine proteases family which induces apoptosis through mitochondria-dependent cytochrome c release pathway. This gene also causes apoptosis by chromatin condensation and DNA fragmentation and eventually results in the formation of apoptotic bodies

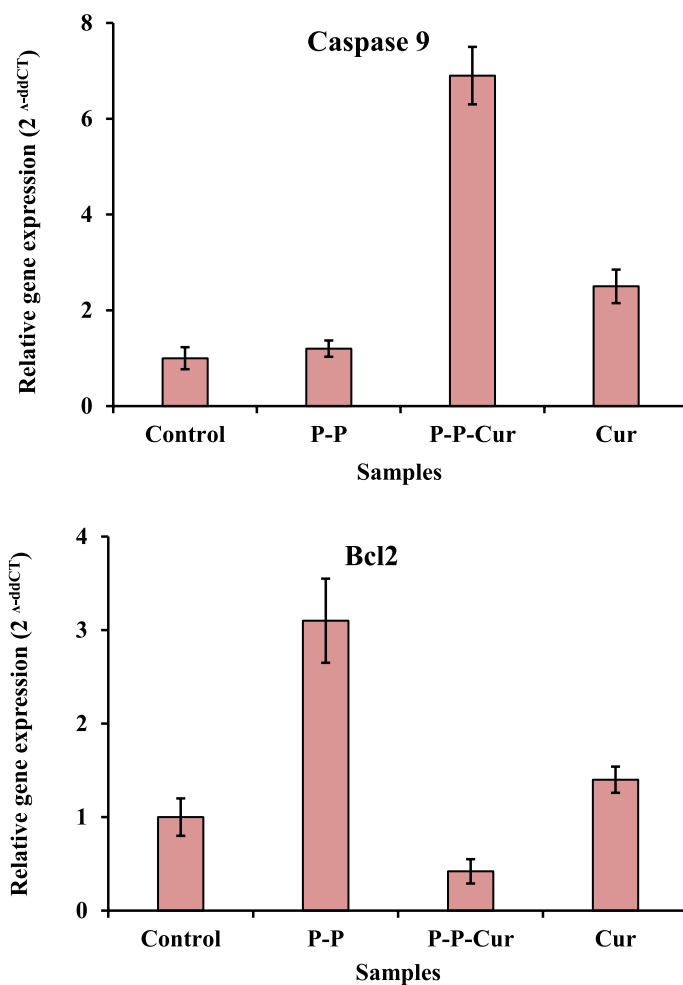


**Fig. 6** The relative gene expression level of caspase-9 and Bcl2 genes after treatment with P-P, P-P-Cur, and Cur samples in A549 cancer cells. After using IC50 concentrations of P-P-Cur and Cur samples, the increase of 7-fold and 2.5-fold is seen in expression levels of caspase9, respectively. The expression level of Bcl2 is considerably decreased by more than 2-fold after treatment with P-P-Cur, whereas the reverse is true for the P-P sample (rise to 3-fold) which shows biocompatibility of copolymerized sample. \* $P < 0.05$ , \*\* $P < 0.01$ , \*\*\* $P < 0.001$ , \*\*\*\* $P < 0.0001$

in cancer cells (Sharifi et al. 2015). On the other hand, Bcl2, which regulates and mediates apoptosis in cancer cell through the mechanism by which mitochondria contribute to the intrinsic apoptosis pathway, has one of the main roles in the fate of cancer cells (Czabotar et al. 2014). From Fig. 6, it can be seen that although pure Cur is led to enhancement in the expression of Bcl2, the reverse result is true regarding the P-P-Cur sample (as half as the control group). P-P nanobeads have also raised the expression of Bcl2 up to 3-fold which is assigned to the biocompatibility of copolymerized nanocarrier (Fotouhi et al. 2021).

#### Cellular uptake

To evaluate the internalization values of the P-P-Cur nanobeads in A549 cells, the flow cytometry approach was performed. Investigating the efficiency of cellular

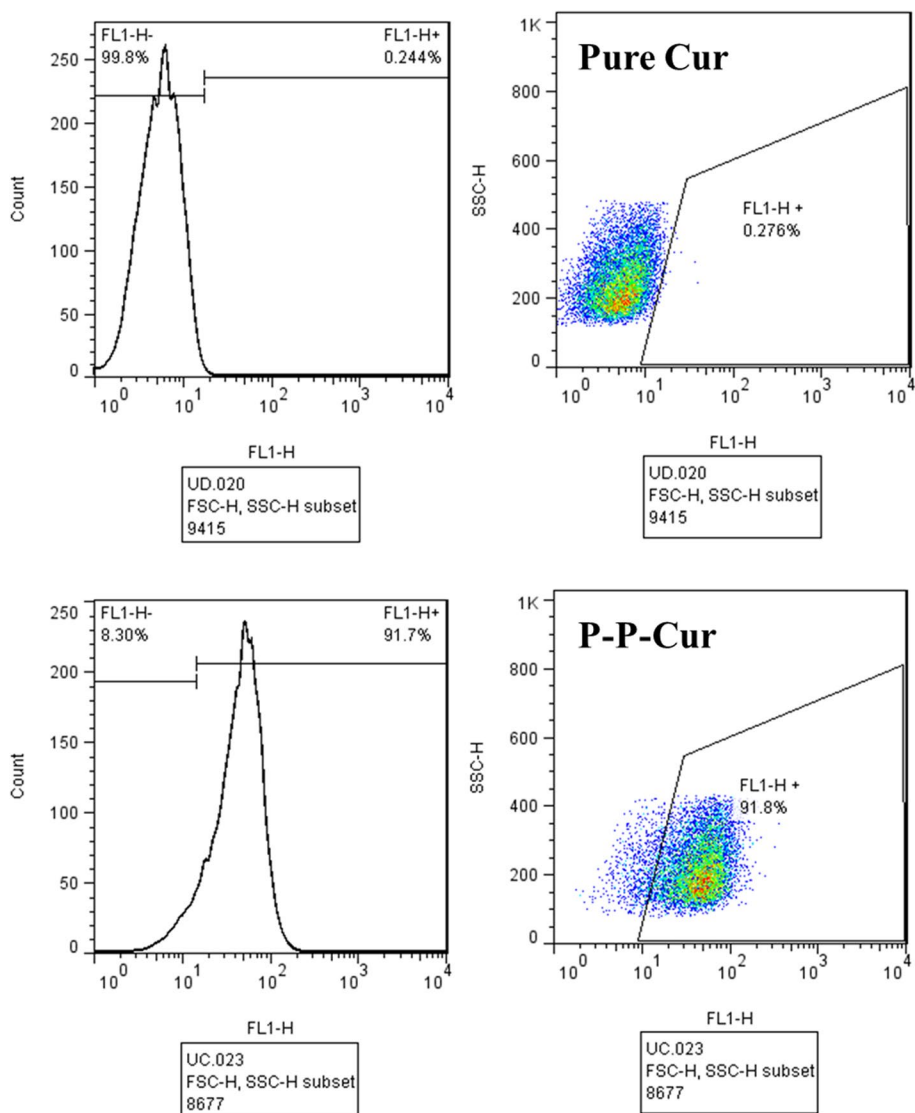


**Fig. 7** Cellular uptake results applying the flow cytometry technique. The internalization of P-P-Cur in the cancer cells is 91.8% after 5 h of treatment while it is less than 1% for pure Cur which shows the effect of P-P in solubilizing and internalizing Cur in target cells

uptake is one of the most important techniques in figuring out the potency of nano-carrier in targeting cancer cells (Zhang et al. 2018; Gunathilake et al. 2022). The results of this test which is done by applying the FITC-labeled nanobeads are demonstrated in Fig. 7. Internalization of nano-sized material can be carried out through the EPR effect and pinocytosis in target tissue and cells which approves the effective targeting of cancer cell compared to conventional approach such as chemotherapy (Birk et al. 2021). On the other hand, since the metabolic rate of cancer cells is higher than normal cells, the internalization efficiency of nanodevice in cancer cells occurs at a high level. According to the results, 91.8% internalization is attained after 5 h of treatment with 100 nM concentrations of nanocarrier which approves the efficient cellular uptake of DDS in the target cells. The internalization of pure Cur is considerably

lower than that of nanobeads which could be due to the insolubility of Cur in hydrophilic mediums which, in turn, reduces its internalization in target cells (Carvalho, D.d.M. et al. 2015). There are several possible pathways for the endocytosis of micro-/ nano-sized drug delivery systems in cancer cells. The major pathways include clathrin/caveolar-mediated endocytosis, phagocytosis, macropinocytosis, and pinocytosis. The size and the shape of nanocarriers are associated with the type of endocytosis as the globular nanocarriers indicated faster endocytosis than non-globular and tubular nanocarriers. Non-globular nanocarriers have higher cytotoxicity than globular nanocarriers since they have poor endocytosis and are vastly exposed to blood flow (Detampel et al. 2022). Besides, the large-sized nanocarriers (about 120 nm) could be internalized through the clathrin-dependent pathway to the target cells. On the other hand, while the clathrin-mediated endocytosis is involved in the endocytosis of nanocarriers with a size of about 100 nm, the caveola-mediated endocytosis is responsible for the internalization of nanocarriers with a size range from 60 to 90 nm. Generally, large-in-size nanocarriers can be internalized to cancer cells through phagocytosis and non-specific macropinocytosis (300–1000 nm) (Bannunah 2024). Moreover, pinocytosis takes place for the internalization of nanocarriers with a smaller size than those done during phagocytosis. As a result, it is possible for our synthesized nanobeads to be internalized through clathrin-dependent, micropinocytosis, and phagocytosis. The results of our work are relatively in consistent with a work by Mukhopadhyay et al. (2020). They have developed folic acid-functionalized PLGA-based DDS for targeted delivery of gemcitabine and Cur to breast cancer cells and based on their results, the internalization of Cur-loaded nanocarrier was about 20-fold higher than that of pure Cur which indicated the impact of polymeric DDS in enhancing the internalization of hydrophobic therapeutics (Mukhopadhyay et al. 2020).

## Conclusion

In the present research, the Cur-entrapped copolymerized P-P nanobeads were fabricated as a kind of biocompatible and efficient DDS against A549 lung cancer cells. The synthesized nanobeads were analyzed applying analytical devices, including FT-IR, DLS, TGA, and TEM, and the physicochemical aspects of nanobeads were determined. As nano-metric size, suitable drug entrapment efficiency, and controlled and pH-sensitive drug release behavior were observed for P-P-Cur nanocomposites. Afterward, different biomedical assays, including cell viability (MTT), gene expression, cell cycle arrest, and cellular uptake were conducted to evaluate the lung cancer cell inhibition ability and apoptosis-inducing potency of the synthesized DDS. Biomedical tests have indicated that P-P-Cur can effectively suppress A549 lung cancer cells and induce apoptosis more efficiently than pure Cur which is relatively insoluble in aqueous mediums. These data have exhibited that while the expression of anti-apoptotic gene decreases, apoptosis gene expression increases after treatment with P-P-Cur, and cellular uptake of Cur raises when exposures to cancer cells in the form of loaded in copolymerized nanocarrier. Totally, these outputs have presented that the fabricated nanobeads would be an excellent candidate for the treatment of lung cancer, and can replace with conventional approaches in cancer therapy.

### Author contributions

All authors reviewed the manuscript.

### Declarations

#### Competing interests

The authors declare no competing interests.

Received: 30 October 2023 Accepted: 16 June 2024

Published online: 24 June 2024

### References

- Abdous H et al (2023) Green synthesis of chitosan/polyacrylic acid/graphitic carbon nitride nanocarrier as a potential pH-sensitive system for curcumin delivery to MCF-7 breast cancer cells. *Int J Biol Macromol* 242:125134
- Abou-ElNour M et al (2019) Triamcinolone acetonide-loaded PLA/PEG-PDL microparticles for effective intra-articular delivery: synthesis, optimization, in vitro and in vivo evaluation. *J Control Release* 309:125–144
- Abrisham M et al (2020) The role of polycaprolactone-triol (PCL-T) in biomedical applications: a state-of-the-art review. *Eur Polymer J* 131:109701
- Alizadeh N, Malakzadeh S (2020) Antioxidant, antibacterial and anti-cancer activities of  $\beta$ - and  $\gamma$ -CDs/curcumin loaded in chitosan nanoparticles. *Int J Biol Macromol* 147:778–791
- Almajidi YQ et al (2023) Advances in chitosan-based hydrogels for pharmaceutical and biomedical applications: a comprehensive review. *Int J Biol Macromol* 253:127278
- Almajidi YQ et al (2024) Chitosan-based nanofibrous scaffolds for biomedical and pharmaceutical applications: a comprehensive review. *Int J Biol Macromol* 264:130683
- Almurshedi AS et al (2018) A novel pH-sensitive liposome to trigger delivery of afatinib to cancer cells: impact on lung cancer therapy. *J Mol Liq* 259:154–166
- Amirishoar M et al (2023) Design and fabrication of folic acid-conjugated and gold-loaded poly (lactic-co-glycolic acid) biopolymers for suppression of breast cancer cell survival combining photothermal and photodynamic therapy. *J Drug Deliv Sci Technol* 83:104266
- Avramović N et al (2020) Polymeric nanocarriers of drug delivery systems in cancer therapy. *Pharmaceutics* 12(4):298
- Banimohamad-Shotorbani B et al (2021) The efficiency of PCL/HAp electrospun nanofibers in bone regeneration: a review. *J Med Eng Technol* 45(7):511–531
- Bannunah A et al (2024) Difference in endocytosis pathways used by differentiated versus nondifferentiated epithelial caco-2 cells to internalize nanosized particles. *Mol Pharm*. <https://doi.org/10.1021/acs.molpharmaceut.4c00333>
- Benkaddour A et al (2013) Grafting of polycaprolactone on oxidized nanocelluloses by click chemistry. *Nanomaterials* 3(1):141–157
- Birk SE, Boisen A, Nielsen LH (2021) Polymeric nano- and microparticulate drug delivery systems for treatment of biofilms. *Adv Drug Deliv Rev* 174:30–52
- Carolina Alves R et al (2019) A critical review of the properties and analytical methods for the determination of curcumin in biological and pharmaceutical matrices. *Crit Rev Anal Chem* 49(2):138–149
- Chen S et al (2016) Targeting tumor microenvironment with PEG-based amphiphilic nanoparticles to overcome chemoresistance. *Nanomed: Nanotechnol, Biol Med* 12(2):269–286
- Ching YC et al (2019) Curcumin/Tween 20-incorporated cellulose nanoparticles with enhanced curcumin solubility for nano-drug delivery: characterization and in vitro evaluation. *Cellulose* 26(9):5467–5481
- Clinton SK, Giovannucci EL, Hursting SD (2020) The world cancer research fund/American institute for cancer research third expert report on diet, nutrition, physical activity, and cancer: impact and future directions. *J Nutr* 150(4):663–671
- Czabotar PE et al (2014) Control of apoptosis by the BCL-2 protein family: implications for physiology and therapy. *Nat Rev Mol Cell Biol* 15(1):49–63
- Dandamudi M et al (2021) Chitosan-coated PLGA nanoparticles encapsulating triamcinolone acetonide as a potential candidate for sustained ocular drug delivery. *Pharmaceutics*. <https://doi.org/10.3390/pharmaceutics13101590>
- de Carvalho DM et al (2015) Production, solubility and antioxidant activity of curcumin nanosuspension. *Food Sci Technol* 35:115–119
- Debele TA et al (2020) Combination delivery of alpha-tocopheryl succinate and curcumin using a GSH-sensitive micelle (PAH-SS-PLGA) to treat pancreatic cancer. *Pharmaceutics*. <https://doi.org/10.3390/pharmaceutics12080778>
- Deng H et al (2019) Injectable thermosensitive hydrogel systems based on functional PEG/PCL block polymer for local drug delivery. *J Control Release* 297:60–70
- Detampel P et al (2022) Caveolin-initiated macropinocytosis is required for efficient silica nanoparticles' transcytosis across the alveolar epithelial barrier. *Sci Rep* 12(1):9474
- Dethe MR et al (2022) PCL-PEG copolymer based injectable thermosensitive hydrogels. *J Control Release*. <https://doi.org/10.1016/j.jconrel.2022.01.035>
- Farghadani R, Naidu R (2021) Curcumin: modulator of key molecular signaling pathways in hormone-independent breast cancer. *Cancers* 13(14):3427
- Fotouhi P et al (2021) Surface modified and rituximab functionalized PAMAM G4 nanoparticle for targeted imatinib delivery to leukemia cells: in vitro studies. *Process Biochem* 111:221–229
- Ghitman J et al (2020) Review of hybrid PLGA nanoparticles: future of smart drug delivery and theranostics medicine. *Mater Des* 193:108805

- Gunathilake TMSU et al (2022) Enhanced curcumin loaded nanocellulose: a possible inhalable nanotherapeutic to treat COVID-19. *Cellulose* 29(3):1821–1840
- Hadar J et al (2019) Characterization of branched poly (lactide-co-glycolide) polymers used in injectable, long-acting formulations. *J Control Release* 304:75–89
- He B et al (2020) A machine learning framework to trace tumor tissue-of-origin of 13 types of cancer based on DNA somatic mutation. *Biochim Et Biophys Acta (BBA) - Mol Basis Dis* 1866(11):165916
- Ion D et al (2021) An up-to-date review of natural nanoparticles for cancer management. *Pharmaceutics* 14(1):18
- Jiang M et al (2023) Advances in preparation, biomedical, and pharmaceutical applications of chitosan-based gold, silver, and magnetic nanoparticles: a review. *Int J Biol Macromol* 251:126390
- Jusu SM et al (2020) Drug-encapsulated blend of PLGA-PEG microspheres: in vitro and in vivo study of the effects of localized/targeted drug delivery on the treatment of triple-negative breast cancer. *Sci Rep* 10(1):14188
- Khakinahad Y et al (2022) Margetuximab conjugated-PEG-PAMAM G4 nano-complex: a smart nano-device for suppression of breast cancer. *Biomed Eng Lett*. <https://doi.org/10.1007/s13534-022-00225-z>
- Kharat M et al (2017) Physical and chemical stability of curcumin in aqueous solutions and emulsions: impact of pH, temperature, and molecular environment. *J Agric Food Chem* 65(8):1525–1532
- Lu B, Lv X, Le Y (2019) Chitosan-modified PLGA nanoparticles for control-released drug delivery. *Polymers* 11(2):304
- Makadia HK, Siegel SJ (2011) Poly lactic-co-glycolic acid (PLGA) as biodegradable controlled drug delivery carrier. *Polymers* 3(3):1377–1397
- Mariadoss AVA et al (2022) Smart drug delivery of p-coumaric acid loaded aptamer conjugated starch nanoparticles for effective triple-negative breast cancer therapy. *Int J Biol Macromol* 195:22–29
- Mortezaee K et al (2021) Synergic effects of nanoparticles-mediated hyperthermia in radiotherapy/chemotherapy of cancer. *Life Sci* 269:119020
- Moutabian H et al (2022) The cardioprotective effects of nano-curcumin against doxorubicin-induced cardiotoxicity: a systematic review. *BioFactors*. <https://doi.org/10.1002/biof.1823>
- Mukhopadhyay R et al (2020) Gemcitabine co-encapsulated with curcumin in folate decorated PLGA nanoparticles; a novel approach to treat breast adenocarcinoma. *Pharm Res* 37(3):56
- Naderlou E et al (2020) Enhanced sensitivity and efficiency of detection of *Staphylococcus aureus* based on modified magnetic nanoparticles by photometric systems. *Artif Cells, Nanomed, Biotechnol* 48(1):810–817
- Narmani A, Jafari SM (2021) Chitosan-based nanodelivery systems for cancer therapy: recent advances. *Carbohydr Polym* 272:118464
- Narmani A, Yavari K, Mohammadnejad J (2017) Imaging, biodistribution and in vitro study of smart 99mTc-PAMAM G4 dendrimer as novel nano-complex. *Colloids Surf, B* 159:232–240
- Narmani A et al (2018a) Gadolinium nanoparticles as diagnostic and therapeutic agents: their delivery systems in magnetic resonance imaging and neutron capture therapy. *J Drug Deliv Sci Technol* 44:457–466
- Narmani A et al (2018b) Targeting delivery of oxaliplatin with smart PEG-modified PAMAM G4 to colorectal cell line: in vitro studies. *Process Biochem* 69:178–187
- Narmani A et al (2019) Folic acid functionalized nanoparticles as pharmaceutical carriers in drug delivery systems. *Drug Dev Res* 80(4):404–424
- Narmani A et al (2020) Breast tumor targeting with PAMAM-PEG-5FU-99mTc as a new therapeutic nanocomplex: in vitro and in-vivo studies. *Biomed Microdevices* 22(2):31
- Narmani A et al (2023) Smart chitosan-PLGA nanocarriers functionalized with surface folic acid ligands against lung cancer cells. *Int J Biol Macromol* 245:125554
- Palamà IE et al (2017) Therapeutic PCL scaffold for reparation of resected osteosarcoma defect. *Sci Rep* 7(1):1–12
- Patel SS et al (2020) Cellular and molecular mechanisms of curcumin in prevention and treatment of disease. *Crit Rev Food Sci Nutr* 60(6):887–939
- Pelaz B et al (2017) Diverse applications of nanomedicine. *ACS Nano* 11(3):2313–2381
- Rezvani M et al (2018) Synthesis and in vitro study of modified chitosan-polycaprolactam nanocomplex as delivery system. *Int J Biol Macromol* 113:1287–1293
- Saadh MJ et al (2024) Advances in chitosan-based blends as potential drug delivery systems: a review. *Int J Biol Macromol* 273:132916
- Salam A et al (2022) Effect of post-diagnosis exercise on depression symptoms, physical functioning and mortality in breast cancer survivors: a systematic review and meta-analysis of randomized control trials. *Cancer Epidemiol* 77:102111
- Sarani M et al (2024) Green synthesis of Ag and Cu-doped bismuth oxide nanoparticles: revealing synergistic antimicrobial and selective cytotoxic potentials for biomedical advancements. *J Trace Elem Med Biol* 81:127325
- Shakeri A et al (2019) Anti-angiogenic activity of curcumin in cancer therapy: a narrative review. *Curr Vasc Pharmacol* 17(3):262–269
- Sharifi S et al (2015) Doxorubicin changes Bax/Bcl-xL ratio, caspase-8 and 9 in breast cancer cells. *Adv Pharm Bull* 5(3):351–359
- Sheffey WV et al (2022) PLGA's plight and the role of stealth surface modification strategies in its use for intravenous particulate drug delivery. *Adv Healthcare Mater* 11(8):2101536
- Shim MK et al (2022) Tumor-activated carrier-free prodrug nanoparticles for targeted cancer immunotherapy: preclinical evidence for safe and effective drug delivery. *Adv Drug Deliv Rev*. <https://doi.org/10.1016/j.addr.2022.114177>
- Stanicki D et al (2022) An update on the applications and characteristics of magnetic iron oxide nanoparticles for drug delivery. *Expert Opin Drug Deliv* 19(3):321–335
- Taghavi S et al (2017) Chitosan-modified PLGA nanoparticles tagged with 5TR1 aptamer for in vivo tumor-targeted drug delivery. *Cancer Lett* 400:1–8
- Tamaddoni A et al (2020) The anticancer effects of curcumin via targeting the mammalian target of rapamycin complex 1 (mTORC1) signaling pathway. *Pharmacol Res* 156:104798
- Xu J et al (2019) Formulation and characterization of spray-dried powders containing vincristine-liposomes for pulmonary delivery and its pharmacokinetic evaluation from in vitro and in vivo. *J Pharm Sci* 108(10):3348–3358

- Yousefi M, Narmani A, Jafari SM (2020) Dendrimers as efficient nanocarriers for the protection and delivery of bioactive phytochemicals. *Adv Coll Interface Sci* 278:102125
- Yuan S et al (2012) Surface modification of polycaprolactone substrates using collagen-conjugated poly (methacrylic acid) brushes for the regulation of cell proliferation and endothelialisation. *J Mater Chem* 22(26):13039–13049
- Zhang X-P et al (2018) Effect of nanoencapsulation using poly (lactide-co-glycolide) (PLGA) on anti-angiogenic activity of bevacizumab for ocular angiogenesis therapy. *Biomed Pharmacother* 107:1056–1063

### **Publisher's Note**

Springer Nature remains neutral with regard to jurisdictional claims in published maps and institutional affiliations.